NJC

ROYAL SOCIETY OF CHEMISTRY

PAPER

Cite this: *New J. Chem.*, 2023, **47**, 15638

Structure and magnetic characterization of some bicompartmental [N_6O_2] divalent metal(II) complexes using bis(phenolato) ligands bearing two pendant bis(pyridyl) amine arms†

Franz A. Mautner,*[a] Roland C. Fischer,[b] Ana Torvisco,[b] Kai Nakashima,[c] Makoto Handa,[c] Masahiro Mikuriya,[d] Nahed M. H. Salem,[e] Gabriel J. Overby,[f] Madison R. Maier,[f] Febee R. Louka[e] and Salah S. Massoud *[ef]

Reactions of the bicompartmental bis(phenolato) compound 6,6′-methylenebis(2-((bis(pyridin-2-ylmethyl)-amino)methyl)-4-chlorophenol)hemihydrate ($H_2L\ \frac{1}{2}H_2O$) with 3d metal(II) ions afforded novel fully structurally characterized bridged acetato dinuclear complexes $[Mn_2(HL)(\mu_{1,2}\text{-}OAc)_2]PF_6$ (**1**) $[Zn_2(HL)(\mu_{1,2}\text{-}OAc)(H_2O)_{0.75}\text{-}(MeOH)_{0.25}](PF_6)_2{\cdot}0.45(H_2O)$ (**5**) and $[Cd_2(HL)(\mu_{1,1,2}\text{-}OAc)(OAc)(H_2O)]PF_6{\cdot}H_2O$ (**6**) as well as the polymeric bridged-azido tetranuclear *catena*-$[Cu_4(HL)_2(\mu_{1,1}\text{-}N_3)_2(\mu_{1,3}\text{-}N_3)_2](NO_3)_2{\cdot}5H_2O$ (**4**). The complex $[Cu_4(HL)_2(ClO_4)_3\text{-}(H_2O)_5](ClO_4)_3{\cdot}5H_2O$ (**2**) was partially characterized. In addition, three more dinuclear complexes $[Cu_2(H_2L)\text{-}(NO_3)_2(H_2O)_2](NO_3)_2$ (**3**), $[Cu_2(HL)(OAc)(CH_3OH)](PF_6)_2$ (**7**) and $[Cu_2(HL)(NCS)_2]NO_3{\cdot}2H_2O$ (**8**) were also isolated. All complexes were characterized by CHN elemental analysis, IR and UV-Vis spectroscopy, ESI-MS, conductivity measurements and X-ray single crystal crystallography for compounds **1**, **4**, **5** and **6**, where the bis(phenolato) ligand displayed different deprotonation (H_2L, HL^- and L^{2-}). The magnetic susceptibility measurements over the temperature range 2–300 K revealed very weak antiferromagnetic coupling in dimanganese(II) **1** (J = −1.64(1) cm^{-1}) and almost negligible magnetic interaction in dicopper(II) **2** (J = 0(3) cm^{-1}). In the azido *catena*-$[Cu_4(HL)_2(\mu_{1,1}\text{-}N_3)_2(\mu_{1,3}\text{-}N_3)_2](NO_3)_2{\cdot}5H_2O$ (**4**) complex, the J value of −133(3) cm^{-1} was obtained upon moderate-to-strong antiferromagnetic coupling through the di-$\mu_{1,3}$-N_3-bridged dicopper(II) unit with no magnetic interaction between the two copper(II) ions in the di-$\mu_{1,1}$-N_3-bridged unit.

Received 24th May 2023,
Accepted 20th July 2023

DOI: 10.1039/d3nj02380j

rsc.li/njc

Introduction

Dinuclear metal complexes have been employed for a long time to mimic the mechanistic pathways for metalloenzymes, catecholase oxidases,[1,2] metallo-β-lactamases (MβL),[3] hemocyanin,[4] DNA and RNA cleavage,[5–7] hydrolysis of phosphodiesters[8] and purple acid phosphatases[9] and as anticancer agents.[10] These molecules have been widely used to monitor and elucidate the spectroscopic structural features in many biological systems. Some dinuclear dioxido-bridged complexes of Mn, Fe, Cu and Ni were reported to activate oxygen insertion in the aliphatic and aromatic compounds' C–H bonds reactions (monooxygenase).[11,12] Moreover, di-nuclear 3d metal complexes have potential applications as catalysts, oxidizing agents,[13,14] and electrochemical and photochemical catalysts for the oxidation of alcohol, ether and water.[14–16] Another feature of these complexes is their use in the field of materials science for molecular magnetism,[17–20] where some of these compounds were shown to behave as single molecule magnets (SMMs).[16,21,22] Also, heteronuclear transition metal-lanthanides, 3d–4f complexes derived from Schiff bases containing phenolic and alkoxy groups, have the capability of fixing atmospheric CO_2.[21]

[a] *Institut für Physikalische and Theoretische Chemie, Technische Universität Graz, Stremayrgasse 9/II, A-8010, Graz, Austria. E-mail: mautner@tu-graz.at; Fax: +43 316-4873-8225; Tel: +43 316-873-8234*
[b] *Institut für Anorganische Chemie, Technische Universität Graz, Stremayrgasse 9, A-8010 Graz, Austria*
[c] *Department of Chemistry, Interdisciplinary Graduate School of Science and Engineering, Shimane University, 1060 Nishikawatsu, Matsue 690-8504, Japan*
[d] *Department of Applied Chemistry for Environment, School of Biological and Environmental Sciences, Kwansei Gakuin University, 1 Gakuen Uegahara, Sanda 669-1330, Japan*
[e] *Department of Chemistry, Faculty of Science, Alexandria University, Moharam Bey, 21511 Alexandria, Egypt. E-mail: ssmassoud@louisiana.edu*
[f] *Department of Chemistry, University of Louisiana at Lafayette, P.O. Box 43700 Lafayette, LA 70504-4370, USA. Fax: +1 337-482-5676; Tel: +1 337-482-5672*

† Electronic supplementary information (ESI) available: ESI-MS and NMR spectra of the ligand are presented in Fig. S1 and S2, respectively. ESI-MS spectra of complexes **2–8** are presented in Fig. S3–S9, respectively. Selected bond parameters (Table S2), hydrogen bond systems (Table S3), non-covalent ring–ring interactions (Table S3), packing plots (Fig. S10–S13) and perspective views of complex units in **2** (Fig. S14a, S14b). CCDC Deposition numbers CCDC 2264307–2264310 for **1**, **4**, **5** and **6**, respectively. For ESI and crystallographic data in CIF or other electronic format see DOI: **https://doi.org/10.1039/d3nj02380j**

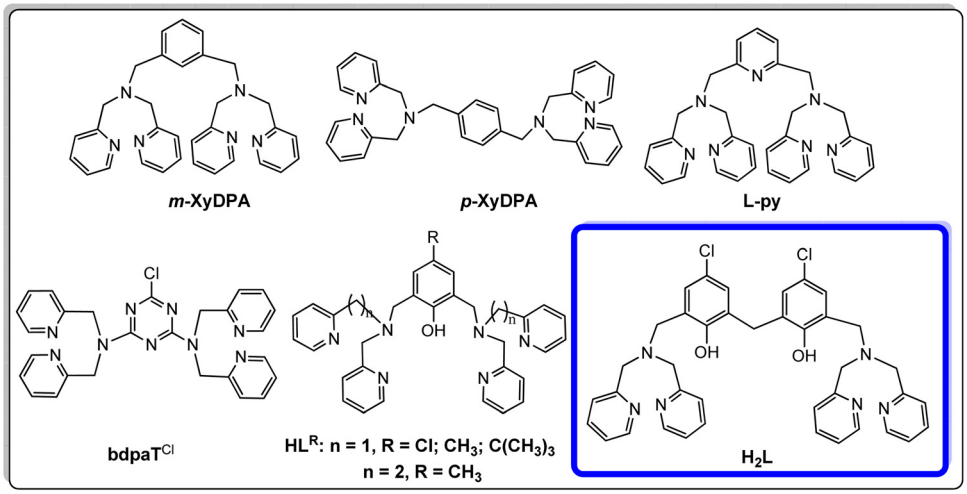

Scheme 1 Structural formulas of some bicompartmental amine ligands and their abbreviations.

Binucleating compounds bearing bis(pyridyl) groups assembled through *m*- or *p*-xylyl, pyridyl,[20,23,24] 1,3,5-triazine[6] and in particular mono-phenolate spacers[2,7,8,10,12,17–19,25] have been reported (Scheme 1). Obviously, each of the pendant pyridyl arms in these molecules binds a metal ion (M^{2+} or M^{3+}) leading to the formation of dinuclear species, which in some ligands may have an extra coordination donor atom (Scheme 1: L-py, $bdpaT^{Cl}$, and HL^{R}). This property is well pronounced in binucleating compounds containing phenolate as a spacer group (Scheme 1: HL^{R}). In this class of phenolate derivatives, dinuclear bridging bimetallic complexes are obtained and in most cases through deprotonated phenolate (phenoxido groups) or neutral phenolate like μ-phenoxido groups.[2,7,8,10,12,17–19,25] However, in the presence of other small bridging groups, such as hydroxide, oxide, peroxide, pseudohalides and acetate, and due to the close proximity between the two metal centers, doubly homoletically bridged metal complexes like di-μ-phenoxido, di-μ-hydroxido and di-μ-oxido, or doubly heterolytically bridged metal complexes like μ-phenoxido-μ-pseudohalide are produced.[5b,7,12d,19,25–27]

Herein we report the synthesis of a novel bicompartmental bis(phenolato) compound containing two pendant bis(pyridyl)-amine arms, namely 6,6′-methylenebis(2-((bis(pyridin-2-ylmethyl)amino)-methyl)-4-chlorophenol)hemihydrate, $H_2L{\cdot}\frac{1}{2}H_2O$, where the two bis(pyridyl)phenolate moieties are separated from each other by the CH_2 group (Scheme 1). As a result, the two phenolates exhibit magnetically independent behavior, except in the presence of bridging groups. The coordination chemistry of the ligand is investigated with various divalent metal ions: Mn^{2+}, Cu^{2+}, Zn^{2+} and Cd^{2+}. The complexes are spectroscopically and structurally characterized and their magnetic properties are examined when coordinated to paramagnetic ions.

Results and discussion

Synthetic aspects

The synthesis of bicompartmental bis(phenolato) compound 6,6′-methylenebis(2-((bis(pyridin-2-ylmethyl)amino)methyl)-4-chlorophenol)hemihydrate ($H_2L{\cdot}\frac{1}{2}H_2O$, Scheme 1) was straight forward through the hydroformylation of 2,2′-methylenebis(4-chlorophenol) with two equivalents of an aqueous solution of 37% HCHO and Et_3N in MeOH. Each of the phenolate groups, separated by a CH_2 group is connected to two pendant bis(pyridyl)amine arms. The structural feature of the ligand indicates that the phenolate groups should act independent of each other, unless small bridging ligands may be present in the reaction with possible partial or complete deprotonation of the phenolate moieties. The UV spectrum of H_2L obtained in MeOH shows three strong λ_{max} at 213, 262 and 294 nm corresponding to the ligand electronic transitions σ–σ*, π–π* and n–π*, respectively. The ESI-MS spectra of the ligand in CH_3OH revealed a single peak at m/z = 691.2356 (100%), corresponding to the protonated ligand ($H_2L + H^+$) (m/z = 691.2355) (Fig. S1, ESI†). The ^1H and ^{13}C NMR (Fig. S2, ESI†) assignments of the ligand H_2L are shown in Scheme 2.

Reaction of a methanolic solution containing $H_2L{\cdot}\frac{1}{2}H_2O$ and two molar amounts of $Cu(ClO_4)_2{\cdot}6H_2O$ and Et_3N resulted in the formation of dinuclear species $[Cu_2(HL)(ClO_4)_2(H_2O)_2]ClO_4{\cdot}3H_2O$ (**2**), in which the perchlorato ligands are mono coordinated to each Cu(II) ion. The dinuclear compound, $[Cu_2(H_2L)(NO_3)_2(H_2O)_2](NO_3)_2$ (**3**) was also isolated when $Cu(NO_3)_2{\cdot}3H_2O$ was used, but the phenolate groups were fully protonated in this case. However, the reaction conducted with $M(OAc)_2{\cdot}nH_2O$ afforded dinuclear doubly bridged acetato $[Mn_2(HL)(\mu_{1,2}\text{-}OAc)_2]PF_6$ (**1**) as well as the mono-bridged acetato $[Zn_2(HL)(\mu_{1,2}\text{-}OAc)(H_2O)_{0.75}(MeOH)_{0.25}](PF_6)_2{\cdot}0.45(H_2O)$ (**5**) and $[Cd_2(HL)(\mu_{1,1,2}\text{-}OAc)(OAc)(H_2O)]PF_6{\cdot}H_2O$ (**6**) complexes. On the other hand, performing the reaction of complex **3** in the presence of an aqueous solution of NaN_3 afforded the interesting polymeric 1D chain compound based on the tetranuclear *catena*-$[Cu_4(HL)_2(\mu_{1,1}\text{-}N_3)_2(\mu_{1,3}\text{-}N_3)_2](NO_3)_2{\cdot}5H_2O$ (**4**) with alternative doubly bridged end-on ($\mu_{1,1}$-N_3) and end-end ($\mu_{1,3}$-N_3) bridging modes. A similar azido bonding mode was also found in 1D *catena*-$[Cd_2(Et_3en)_2(\mu_{1,1}\text{-}N_3)_2(\mu_{1,3}\text{-}N_3)_2]$ (Et_3en = *N*,*N*,*N*′-triethylethylenediamine).[28] Two more Cu(II) complexes $[Cu_2(HL)(OAc)(CH_3OH)](PF_6)_2$ (**7**) and $[Cu_2(HL)(NCS)_2]NO_3{\cdot}2H_2O$ (**8**) were also synthesized. Although two equivalents of the Et_3N

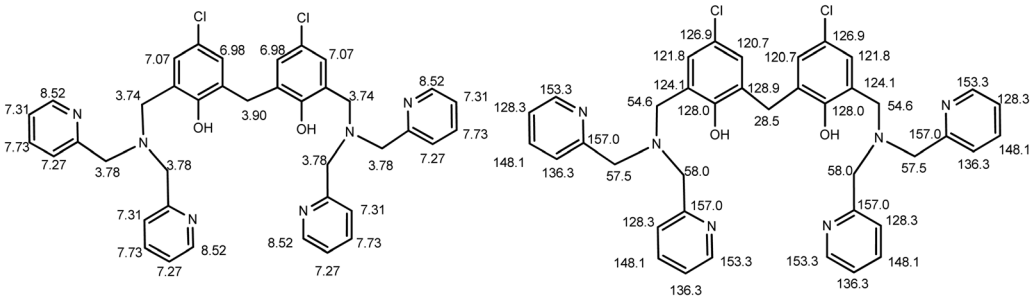

Scheme 2 ^{1}H and ^{13}C NMR assignments of the bis(phenolate) ligand H_2L.

base were employed in all reactions to assist the deprotonation of the phenolate groups, only one was deprotonated in most products (**1**, **2**, **4–8**); probably this may be attributed to the relatively strong hydrogen bonds generated from the deprotonated and protonated phenolates phO···H···Oph. This intra O–H···O hydrogen bonds were demonstrated in complexes **1**, and **4–6** (see the X-ray section). However, we should mention that in complex **3**, the bis(phenolate) ligand reacted in the fully protonated neutral form, H_2L.

The structural features of the isolated complexes were established by elemental microanalyses, ESI-MS, IR and UV-Vis spectroscopy, conductivity measurements and single crystal X-ray crystallography for **1**, **4–6** compounds.

IR spectra

The IR spectra of the investigated complexes and their parent ligand revealed some general characteristic features including broad weak to very weak intense bands over the range 3610–3380 cm^{-1}, characteristic for the ν(O–H) stretching frequency of the coordinated aqua or lattice water molecules in **2–6** and **8** or coordinated CH_3OH in **7**. The bis(phenolate) ligand, H_2L and all its complexes **1–8** exhibit a series of very weak vibrations over the 3040–2900 cm^{-1} region assigned to the ν(C–H) stretching frequencies of the aromatic and aliphatic groups. In addition, all compounds display a symmetrical series of four bands of strong to medium intensity in the 1600–1415 cm^{-1} region, characteristic to the bis(pyridyl) group.[29,30] The perchlorato complex $[Cu_2(HL)(ClO_4)_2(H_2O)_2]ClO_4{\cdot}3H_2O$ (**2**) displayed two strong absorption bands 1068 and 1056 cm^{-1}, attributable to the ν(Cl–O) stretching frequency of the counter and coordinated ClO_4^- groups. The hexafluorophosphate compounds **1**, **5**, **6** and **7** revealed the strong characteristic stretching frequency ν(F-P) of the PF_6^- ion around 930 cm^{-1}. The strong bands observed in the range 1320–1275 cm^{-1} are attributed to the ν(N–O) stretching frequency in the nitrate compounds **3**, **4** and **8**. The azido compound $[Cu_4(HL)_2(\mu_{1,1}\text{-}N_3)_2(\mu_{1,3}\text{-}N_3)_2](NO_3)_2{\cdot}5H_2O$ (**4**) exhibited strong bands at 2040 and 2022 cm^{-1}, whereas the thiocyanato compound $[Cu_2(HL)(NCS)_2]NO_3{\cdot}2H_2O$ (**8**) revealed a strong single band at 2083 cm^{-1}. These bands can be assigned to the asymmetric stretching frequencies $\nu_{as}(N_3^-)$ and $\nu_{as}(NCS^-)$, respectively. The split bands in the azido compound are mainly due to the presence of the azido groups in two different bonding modes, $\mu_{1,1}$-N_3 and $\mu_{1,3}$-N_3. Taking this into consideration, the high preference of Cu^{2+} binds the nitrogen site in the vast majority of mononuclear Cu-thiocyanato complexes, which in most cases show an absorbance band at a frequency lower than 2000 cm^{-1}, whereas the corresponding *S*-NCS bonding, and in some cases, bridged $\mu_{N,S}$-NCS, shows a frequency higher than 2000 cm^{-1}.[31,32] Thus, based on this criterion and the observed $\nu_{as}(NCS^-)$ for complex **8** at 2083 cm^{-1}, one can consider that the thiocyanates undergo *N*-NCS Cu^{2+} bonding.[31,32] The very close IR spectral pattern of the complex cation of $[Cu_2(HL)(OAc)(CH_3OH)](PF_6)_2$ (**7**) to the corresponding structurally determined acetato complexes **1** and **5** may suggest a similar acetate bonding mode, therefore, we tentatively suggest the structural formula of **7** as $[Cu_2(HL)(\mu_{1,2}\text{-}OAc)(CH_3OH)](PF_6)_2$.

Conductivity measurements

In order to explore the electrolytic nature of the complexes under investigation, their molar conductivities Λ_M were measured whenever their solubility permits, and the values are collected in Table 1. The complexes **1**, **4**, **6** and **8** reveal Λ_M values in the range of 128–153 Ω^{-1} cm^2 mol^{-1}, which are in complete agreement with 1 : 1 electrolytic nature. The tetranuclear *catena*-$[Cu_4(HL)_2(\mu_{1,1}\text{-}N_3)_2(\mu_{1,3}\text{-}N_3)_2](NO_3)_2{\cdot}5H_2O$ (**4**) most likely dissociates into two dimeric species, $[Cu_2(HL)(N_3)_2]NO_3$. On the other hand, Λ_M values in the range of 187–272 Ω^{-1} cm^2 mol^{-1} were determined in complexes **2**, **3**, **5** and **7**, indicating 1 : 2 electrolytic behavior as expected based on their molecular formulas.[33] Also, in the case of $[Cu_4(HL)_2(ClO_4)_3(H_2O)_5](ClO_4)_3{\cdot}5H_2O$ (**2**), which consists of two independent crystallographic units $\{[Cu_2(HL)(ClO_4)_2(H_2O)_2]ClO_4$ and $[Cu_2(HL)(ClO_4)(H_2O)_3](ClO_4)_2\}{\cdot}5H_2O$, it seems behaving as a 1 : 2 electrolyte through the release and/or substitution of one coordinated ClO_4^- ligand from the former unit, and the formation of $[Cu_2(HL)(ClO_4)(H_2O)_2]^2 + 2ClO_4^-$ species in the CH_3CN solution.

UV-Vis spectra

The electronic spectra of Cu(II)-H_2L complexes, **2–4**, **7** and **8** obtained in CH_3CN or CH_3OH tabulated in Table 1 exhibit a general spectral pattern for the presence of a low energy single broad band over the wavelength region 640–720 nm. Although this spectral feature may indicate five-coordinate Cu(II) complexes in a distorted square pyramidal geometry (SP),[30,34,35] we still cannot exclude the possibility of a distorted octahedral environment.[36] This band, which is insensitive to the solvent

Table 1 The UV-Vis spectra and molar conductivity, Λ_M of M(II)-H_2L complexes in different solvents

Complex	Solvent	Visible spectrum: λ_{max}, nm (ε_{max} M^{-1} cm^{-1} per Cu atom)	Λ_M (Ω^{-1} cm^2 mol^{-1})
$[Cu_4(HL)_2(ClO_4)_3(H_2O)_5](ClO_4)_3{\cdot}5H_2O$ (**2**)	CH_3CN	714 (123.3)	243.5
$[Cu_2(H_2L)(NO_3)_2(H_2O)_2](NO_3)_2$ (**3**)	CH_3CN		199.2
	CH_3OH	449 (137.5), 655 (90.3)	201.6
	CH_3COCH_3[a]	433, 657	
$[Cu_4(HL)_2(\mu_{1,1}\text{-}N_3)_2(\mu_{1,3}\text{-}N_3)_2](NO_3)_2{\cdot}5H_2O$ (**4**)	CH_3CN[a]	392, 655	
	CH_3OH		127.5
$[Cu_2(HL)(OAc)(CH_3OH)](PF_6)_2$ (**7**)	CH_3OH	431 (213.8), 641 (115.8)	187.3
$[Cu_2(HL)(NCS)_2]NO_3{\cdot}2H_2O$ (**8**)	CH_3CN[a]	374 (m), 483 (sh), 643 (w, b)	
	CH_3OH	370 (914.8), 641 (160.7)	135.4
$[Mn_2(HL)(\mu_{1,2}\text{-}OAc)_2]PF_6$ (**1**)	CH_3OH	510 (sh, w), 565 (vw), ~650 (11.0)	134.6
	CH_3CN	258 (6470), 311 (2850)	139.6
	DMSO	265 (5730), 314 (2635)	
$[Zn_2(HL)(\mu_{1,2}\text{-}OAc)(H_2O)_{0.75}(MeOH)_{0.25}](PF_6)_2{\cdot}0.45(H_2O)$ (**5**)	CH_3OH	255 (sh), 310 (2390, b)	271.0
$[Cd_2(HL)(\mu_{1,1,2}\text{-}OAc)(OAc)(H_2O)]PF_6{\cdot}H_2O$ (**6**)	CH_3OH	259 (sh), 312 (2720)	152.6
	DMSO	263 (7550), 317 (2810)	

[a] Saturated solution.

nature (complexes **3** and **8**), can be assigned to ligand field d–d transition. The strong intense band observed over the region 370–450 nm results from ligand phenolate-oxygen to the Cu(II) ion charge transfer (L → M, CT).[18,26,37,38] The electronic spectra of $[Mn_2(HL)(\mu_{1,2}\text{-}OAc)_2]PF_6$ (**1**) in MeOH revealed a series of very weak bands at 510, 565 and ~650 nm due to Laporte and spin-forbidden transitions.[36] In addition, all complexes and specifically **1**, **5** and **6** showed very strong bands around 260 and 310 nm. These bands were located at comparable positions to those detected in the free ligand, H_2L and attributed to π–π* and n–π* transitions, respectively. Electronic spectra and molar conductivity of complexes are compiled in Table 1.

Mass spectra of the complexes

The ESI-MS measurements of the complexes, performed in acetonitrile (CH_3CN), provide some information about their coordination feature. The mass spectra of the structurally characterized acetato compounds $[Mn_2(HL)(\mu_{1,2}\text{-}CH_3COO)_2]PF_6$ (**1**), $[Zn_2(HL)(\mu_{1,2}\text{-}OAc)(H_2O)_{0.75}(MeOH)_{0.25}](PF_6)_2{\cdot}0.45(H_2O)$ (**5**) and $[Cd_2(HL)(\mu_{1,1,2}\text{-}CH_3COO)(CH_3COO)(H_2O)]PF_6{\cdot}H_2O$ (**6**) produced fragments related to the decomposition of the bridged acetate groups through the release of CO, HCO and HCO_2, respectively (Experimental section). A typical mass spectrum is illustrated in Fig. 1 for the release of CO from complex **1**. The release of HCO_2 in $[Cu_2(HL)(CH_3COO)(CH_3OH)](PF_6)_2$ (**7**) most likely indicates similar acetato-bridging too. Similarly, the formation of fragments such as $CuL(ClO_4)_2$, $HCu_2(HL)(NO_3)_2$ and $Cu_2(HL)(N_3)_3$ in $[Cu_2(HL)(ClO_4)_2(H_2O)_2]ClO_4{\cdot}3H_2O$ (**2**), $[Cu_2(H_2L)(NO_3)_2(H_2O)_2](NO_3)_2$ (**3**) and $[Cu_4(HL)_2(\mu_{1,1}\text{-}N_3)_2(\mu_{1,3}\text{-}N_3)_2](NO_3)_2{\cdot}5H_2O$ (**4**), respectivly, as well as the appearance of the fragment $Cu_2(H_2L)(NCS)$ in $[Cu_2(HL)(NCS)_2]NO_3{\cdot}2H_2O$ (**8**) reflects the possible bridging of NCS^- to the Cu^{2+} ions in this complex (Fig. S3–S9, ESI†). Probably, we should mention that attempts made to obtain good quality single crystals of **2**, **3**, **7** and **8** were failed.

Description of the structures

$[Mn_2(HL)(\mu_{1,2}\text{-}OAc)_2]PF_6$ (1). A perspective view of title compound **1** is given in Fig. 2 and selected bond parameters are

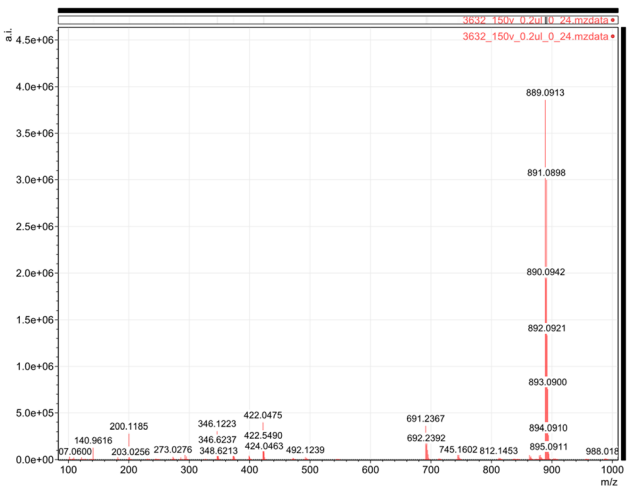

Fig. 1 ESI-MS spectra of $[Mn_2(HL)(\mu_{1,2}\text{-}OAc)_2]PF_6$ (**1**) in acetonitrile.

listed in Table S1 (ESI†). In **1**, the three *N* donor atoms and the phenolato *O* donor atom of each arm of the bicompartmental HL^- anion are ligated to the Mn(II) center to form a dinuclear complex cation, with a Mn···Mn separation of 4.2381(9) Å. The MnN_3O_3 distorted octahedron around the two metal centers is completed by two oxygen atoms of two bridging acetate anions. The Mn–O and Mn–N bond distances vary from 2.073(3) to 2.361(3) Å. The Mn–O–C bond angles of the bridging acetate groups are 140.2(3) and 147.9(3)°. The two phenolato moieties act in protonated and deprotonated forms to create an internal hydrogen bond [O2···O1 = 2.398(4) Å; O2–H···O1 = 172(6)°] (Fig. S10, ESI†). The complex cation of **1** co-crystallizes with a PF_6^- counter anion.

***Catena*-$[Cu_4(HL)_2(\mu_{1,1}\text{-}N_3)_2(\mu_{1,3}\text{-}N_3)_2](NO_3)_2{\cdot}5H_2O$ (4).** Each arm of the two bicompartmental ligands HL in **4** is ligated *via* their three *N*-donors and one phenolato *O*-donor atom to a copper(II) center to form two dinuclear subunits. The elongated octahedra around each of the four metal centers are completed by two N atoms of a pair of bridging azide anions to link the subunits to a 1D polymeric chain (Fig. 3). Within the polymeric

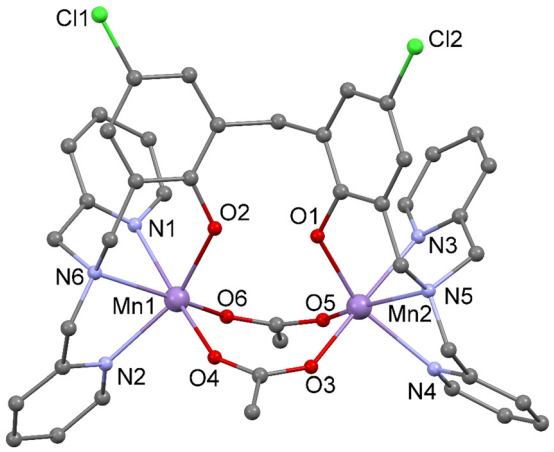

Fig. 2 Coordination figure of the complex cation of **1**.

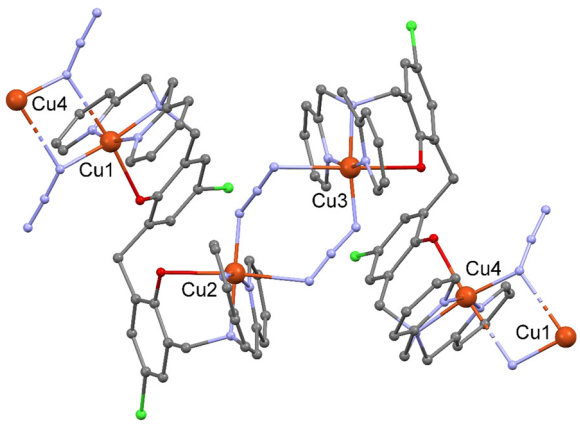

Fig. 3 Perspective view of the polymeric chain of **4**. Color code: brown Cu, green Cl, red O, blue N, black C.

chains, the azide bridges behave in alternate bridging modes: Cu1 and Cu4 centers are linked by two end-on (EO) azide bridges, while Cu2 and Cu3 centers are linked by two end-to-end (EE) azide bridges. The azide bridges are quite asymmetric. Thus, each of the four CuN_5O axially elongated octahedra forms one (semi-coordinative Cu–N(N_3) and one *trans O*-phenolato bond in the range from 2.219(5) to 2.725(5) Å, while the remaining equatorial Cu–N bonds are in the range from 1.942(6) to 2.059(5) Å. The azide groups have N–N bond lengths ranging from 1.137(7) to 1.205(8) Å and N–N–N bond angles from 175.0(6) to 176.2(7)° (Table S1, ESI†). The intra-chain metal···metal separations are 5.9117(11), 5.8776(12), 5.0874(11) and 3.6010(9) Å. The polymeric chains co-crystallize with solvent water molecules and nitrato counter anions. Hydrogen bonds of type O–H···O and O–H···N form a supramolecular 2D system (Fig. S11 and Table S2, ESI†). For charge equilibrium, 50% of the phenolato groups must be protonated and are expected to form intra-chain O–H···O hydrogen bonds with O···O separations of 2.491(6) Å.

$[Zn_2(HL)(\mu_{1,2}\text{-OAc})(H_2O)_{0.75}(MeOH)_{0.25}](PF_6)_2\cdot 0.45(H_2O)$ (5). In **5**, the three *N* donor atoms and the phenolato *O* donor atom

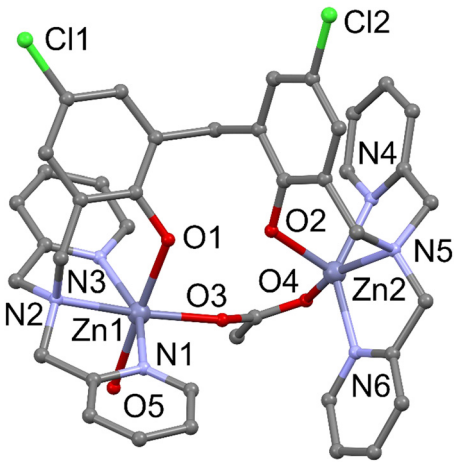

Fig. 4 Coordination figure of the complex cation of **5**. Note: Only O5 of the aqua ligand with occupancy 0.755(15) given, while the terminal methanol molecule with a minor split occupancy of 0.245(15) omitted for clarity.

of each arm of the bicompartmental ligand HL are ligated to a Zn(II) center to form a dinuclear complex cation with a Zn···Zn separation of 4.7318(11) Å. A bridging acetate anion also links the two zinc centers *via* O3 and O4 atoms (Fig. 4). Coordination number six around Zn1 is completed by O5 of a terminal aqua ligand with a major split occupancy of 0.755(15) and by O5A of a terminal methanol molecule with a minor split occupancy of 0.245(15). The penta-coordinated ZnN_3O_2 polyhedron of Zn2 has a distorted square pyramidal geometry with the τ-value[39] of 0.32 and an O2 atom in an apical position. The Zn–O/N bond distances vary from 1.94(4) to 2.241(5) Å. The Zn–O–C bond angles of the bridging acetate group are 120.6(3) and 141.0(4)° (Table S1, ESI†). The two phenolato moieties act in protonated and deprotonated forms to create an internal hydrogen bond [O2···O1 = 2.460(6) Å; O2–H2···O1 = 170(5)°]. The complex cation of **5** co-crystallizes with partially disordered PF_6^- counter anions and a non-coordinated water molecule with an occupancy of 0.453(18).

$[Cd_2(HL)(\mu_{1,1,2}\text{-}CH_3COO)(CH_3COO)(H_2O)]PF_6\cdot H_2O$ (6). This complex behaves in a similar way to **1** and **5**, where the three N donor atoms and the phenolato O donor atom of each arm of the bicompartmental ligand HL^- are ligated to a Cd(II) center to form a dinuclear complex cation, with a Cd···Cd separation of 4.5690(6) Å (Fig. 5). Each Cd center is further ligated by two oxygen atoms of a chelating acetate anion. In addition, acetato oxygen atom O3 is also linked to the Cd2 center. Coordination number seven around Cd1 is completed by O5 of a terminal aqua ligand. The distorted CdN_3O_4 polyhedra around the two metal centers have Cd-N/O bond distances varying from 2.273(2) to 2.698(2) Å. The Cd1–O3–Cd2 bond angle of the bridging acetate group is 135.10(9)° and the two O–Cd–O chelating bond angles are 51.46(7) and 52.25(7)°. The two phenolato moieties act in protonated and deprotonated forms to create an internal hydrogen bond [O1···O2 = 2.470(3) Å; O1–H2···O2 = 172(4)°]. The complex cation of **6** co-crystallizes with a PF_6^- counter anion and a non-coordinated water

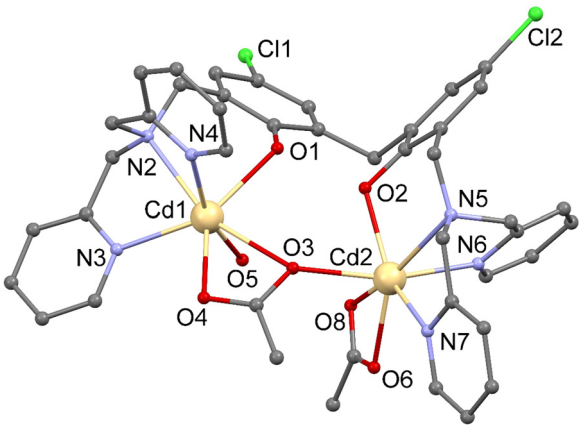

Fig. 5 Coordination figure of the complex cation of **6**.

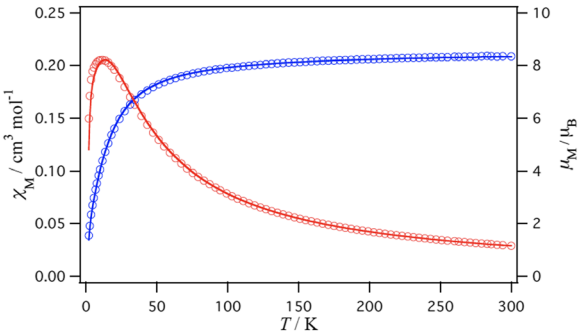

Fig. 6 Temperature dependence of magnetic susceptibility χ_M (○) and magnetic moment μ_M (○) of **1**. The solid lines represent the best fits obtained as described in the text.

molecule. The aqua ligand and water molecule form hydrogen bonds of types O–H···O and O–H···F (Table S2 and Fig. S13, ESI†). Interestingly, the two acetate ligands behave differently, while both of them form four-membered chelate rings to each Cd(II) center, and one of the coordinated *O*-acetato ligands bound to Cd1 is bridged to the Cd2 ion in $\mu_{1,1,2}$-bonding fashion.

Non-covalent ring···ring interactions with Cg···Cg (center of gravity) separations of their aromatic rings less than 3.75 Å are observed in **1** and **5** (Table S3, ESI†).

$[Cu_4(HL)_2(ClO_4)_3(H_2O)_5](ClO_4)_3{\cdot}5H_2O$ (2). The determination of the preliminary structure of this complex showed the presence of two isolated crystallographically independent dimeric $Cu_2(HL)$ units $[Cu_2(HL)(ClO_4)_2(H_2O)_2]ClO_4$ and $[Cu_2(HL)(ClO_4)(H_2O)_3](ClO_4)_2$, in which Cu(II) centers are also ligated by one O phenolato and three N donor atoms of bis(pyridylamine) groups. Octahedral geometry is completed by two terminal aqua ligands for Cu1, while the other three Cu(II) centers are further ligated by one aqua ligand and one terminal $OClO_3$ anion. (ESI,† Fig. S14a and S14b).

Magnetic measurements

$[Mn_2(HL)(\mu_{1,2}\text{-OAc})_2]PF_6$ (1). The magnetic susceptibility data of **1** were measured in the temperature range 2–300 K. Fig. 6 shows the temperature dependence of molar magnetic susceptibility and molar magnetic moment per dinuclear Mn_2 unit. The magnetic moment at 300 K is 8.34μ_B, which is close to non-interacting two S = 5/2 spins, corresponding to the spin-only value 5.92μ_B for high-spin d^5 Mn(II). The magnetic moment gradually decreases with the lowering of temperature until 50 K and then decreases abruptly to 1.55μ_B at 2 K. This magnetic behavior is characteristic of a pair of weakly antiferromagnetic-coupled manganese(II) ions. The magnetic data were analyzed by the van Vleck equation for two interacting S = 5/2 spins (eqn (1) based on the Heisenberg model, $\mathscr{H} = -2JS_1{\cdot}S_2$:

$$\chi_M = (2Ng^2\mu_B{}^2/kT)\{(55 + 30x^{10} + 14x^{18} + 5x^{24} + x^{28})/(11 + 9x^{10} + 7x^{18} + 5x^{24} + 3x^{28} + x^{30}) \quad (1)$$

where $x = \exp(-J/kT)$ and the other symbols have their usual meanings.[40] The solid lines in Fig. 6 represent the best fits and produced the parameters: g = 2.04 and J = −1.64 cm^{-1}. The obtained J value is comparable to those of di-μ-acetato-μ-phenoxido-bridged dimanganese(II) complexes ($|J|$ = 2.5–6 cm^{-1}),[40–42] di-μ-acetato-μ-aqua-bridged dimanganese(II) complexes ($|J|$ = 1–3 cm^{-1}),[43–45] and tri-μ-acetato-bridged dimanganese(II) complex (J = −1.3 cm^{-1}).[46]

$[Cu_4(HL)_2(ClO_4)_3(H_2O)_5](ClO_4)_3{\cdot}5H_2O$ (**2**) or {$[Cu_2(HL)(ClO_4)_2(H_2O)_2](ClO_4)$, $[Cu_2(HL)(ClO_4)(H_2O)_3](ClO_4)_2$}·$5H_2O$. The crystal structure of this complex showed that there are two crystallographically independent dinuclear copper(II) units composed of $[Cu_2(HL)(ClO_4)_2(H_2O)_2]ClO_4$ and $[Cu_2(HL)(ClO_4)(H_2O)_3](ClO_4)_2$, which are similar to each other in the crystal. Therefore, the complex can be regarded as an essentially dinuclear copper(II) species. The temperature dependence of molar magnetic susceptibility and molar magnetic moment of **2** are illustrated in Fig. 7. The magnetic moment at 300 K is 2.71μ_B, which is close to the non-interacting two S = 1/2 spins, corresponding to the spin-only value 1.73μ_B for d^9 Cu(II). The magnetic moment is almost constant and decreases slightly reaching 2.51μ_B at 2 K upon cooling the sample. The magnetic data were analyzed by the molecular field approximation (eqn (2) for the Bleaney–Bowers equation (eqn (3), taking into consideration the magnetic interaction between the neighboring dinuclear molecules as zJ' (z = number of interacting neighbors):[47a]

$$\chi_M{}' = \chi_M/\{1 - (2zJ'/Ng^2\mu_B{}^2)\chi_M\} \quad (2)$$

$$\chi_M = (2Ng^2\mu_B{}^2/3kT)[\{1 + (1/3)\exp(-2J/kT)\}^{-1} + 2N\alpha \quad (3)$$

where J is the exchange coupling constant for the dicopper(II) molecule and $N\alpha$ is the temperature independent paramagnetism. The best-fitting parameters of solid lines shown in Fig. 7 resulted in g = 2.15(1), J = 0(3) cm^{-1}, $N\alpha$ = 60 × 10^{-6} cm^3 mol^{-1} (fixed) and zJ' = −0.2(13) cm^{-1}. This result shows a very weak magnetic coupling between the two copper(II) ions in accordance with the lack of the bridging group between the metal ions.

The best-fitting parameters of solid lines shown in Fig. 7 resulted in g = 2.15, J = 0.02 cm^{-1}, $N\alpha$ = 60 × 10^{-6} cm^3 mol^{-1}

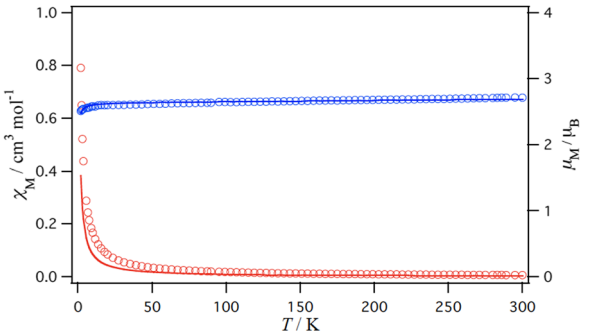

Fig. 7 Temperature dependence of magnetic susceptibility χ_M (○) and magnetic moment μ_M (○) of **2**. The solid lines represent the best fits obtained as described in the text.

(fixed) and $zJ' = -0.20$ cm^{-1}. This result shows a very weak magnetic coupling between the two copper(II) ions in accordance with the lack of the bridging group between the metal ions.

***Catena*-[Cu$_4$(HL)$_2$($\mu_{1,1}$-N$_3$)$_2$($\mu_{1,3}$-N$_3$)$_2$](NO$_3$)$_2$·5H$_2$O (4).** The crystal structure of **4** revealed two kinds of dinuclear molecules: the di-$\mu_{1,1}$-N$_3$-bridged dicopper(II) unit, which exhibits more tendency to ferromagnetic or less likely weak antiferromagnetic coupling, and the di-$\mu_{1,3}$-N$_3$-bridged dicopper(II) unit, which predominantly shows antiferromagnetic coupling. The two dinuclear Cu(II) units are connected by the HL$^-$ ligands to form a zigzag chain of tetranuclear units. This structure may be described as the coexistence of two magnetically different dinuclear copper(II) species in the crystal. Taking into consideration the fact that longer axial coordination is in the range 2.219(5) to 2.725(5) Å, one can ignore the magnetic interaction within the di-$\mu_{1,1}$-N$_3$-bridged dicopper(II) unit. The temperature dependence of molar magnetic susceptibility and molar magnetic moment per tetranuclear Cu$_4$ unit (Fig. 8) reveals molar magnetic moment of 3.86μ_B at 300 K, which corresponds to 1.93μ_B/Cu and close to non-interacting four $S = 1/2$ spins with the spin-only value of 1.73μ_B for d^9 Cu(II). The magnetic moment decreases smoothly with lowering temperature and reaches to 2.61μ_B at 2 K. The magnetic data were analyzed by the molecular field approximation (eqn (4), for the modified Bleaney–Bowers eqn (5) consisting of magnetic interaction in the di-$\mu_{1,3}$-N$_3$-bridged dicopper(II) unit and non-interaction between the two copper(II) ions of the di-$\mu_{1,1}$-N$_3$-bridged dicopper(II) unit,[47] considering the magnetic interaction between the neighboring copper(II) moieties as zJ' (z = number of interacting neighbors):

$$\chi_M' = \chi_M/\{1 - (2zJ'/Ng^2\mu_B^2)\chi_M\} \quad (4)$$

$$\chi_M = (2Ng^2\mu_B^2/3kT)[\{1 + (1/3)\exp(-2J_a/kT)\}^{-1}] + Ng^2\mu_B^2/2kT + 2N\alpha \quad (5)$$

where J is the exchange coupling constant for the di-$\mu_{1,3}$-N$_3$-bridged dicopper(II) unit. The best-fitting parameters (Fig. 8) resulted in $g = 2.39(1)$, $J = -133(3)$ cm^{-1}, $N\alpha = 60 \times 10^{-6}$ cm^3 mol^{-1} (fixed), and $zJ' = -0.44(5)$ cm^{-1}. The obtained J value agrees with observed magnetic coupling *via* the di-$\mu_{1,3}$-N$_3$-bridged dicopper(II) unit.[7]

No attempts were made to determine the magnetic properties of the complexes [Cu$_2$(H$_2$L)(NO$_3$)$_2$(H$_2$O)$_2$](NO$_3$)$_2$·5H$_2$O (**3**), [Cu$_2$(HL)(OAc)(CH$_3$OH)](PF$_6$)$_2$ (**7**) and [Cu$_2$(HL)(NCS)$_2$]NO$_3$·2H$_2$O (**8**) due to the expected weak magnetic coupling between the Cu(II) centers as demonstrated in **2**, and lack of structural information.

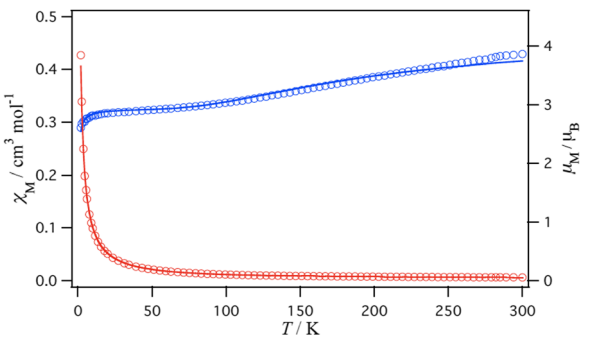

Fig. 8 Temperature dependence of magnetic susceptibility χ_M (○) and magnetic moment μ_M (○) of **4**. The solid lines represent the best fits obtained as described in the text.

Experimental

Materials and physical measurements

2,2′-Methylenebis(4-chlorophenol) was purchased from Alfa Aesar and bis(pyridine-2-ylmethyl)amine (DPA) from TCI America. All other chemicals used in this study were of reagent grade. NMR spectra were collected on a Bruker AvNeo 700 MHz spectrometer at room temperature, whereas ^{13}C NMR spectra were obtained on a Varian 400 NMR spectrometer operating at 100 MHz (^{13}C). Chemical shifts (δ) are reported in ppm and referenced internally to residual solvent resonances (d_6-DMSO: $\delta_H = 2.49$, $\delta_C = 39.4$ ppm) or TMS. ESI-MS spectra of H$_2$L and its M(II) complexes were recorded in CH$_3$OH and CH$_3$CN, respectively on an LC-MS Varian Saturn 2200 Spectrometer. Electronic spectra were recorded using an Agilent 8453 HP diode UV-Vis spectrophotometer. Infrared spectra were recorded on a Cary 630 (ATR-IR) spectrometer. Conductivity measurements were performed using a Mettler Toledo Seven Easy conductivity meter and calibrated by 1413 μS cm^{-1} conductivity standard. The molar conductivity of the complexes was determined from $\Lambda_M = (1.0 \times 10^3\ \kappa)/[M(II)]$, where κ = specific conductance and [M(II)] is the molar concentration of the complex. Elemental analyses were carried out by Atlantic Microlaboratory, Norcross, Georgia, U. S. A.

Caution! Salts of perchlorate and azide and their metal complexes are potentially explosive and should be handled with great care and in small quantities.

Synthesis of the compounds

6,6′-Methylenebis(2-((bis(pyridin-2-ylmethyl)amino)methyl)-4-chlorophenol)hemihydrate (H$_2$L·$\frac{1}{2}$H$_2$O). To a solution containing 2,2′-methylenebis(4-chlorophenol) (0.270 g, 0.01 mol), bis(pyridine-2-ylmethyl)amine (DPA) (4.00 g, 0.02 mol) and triethylamine, Et$_3$N (2.02 g, 0.02 mol) dissolved in 40 mL

MeOH, aqueous 37% HCHO (1.63 g, 0.02) was added. The resulting mixture was refluxed gently for 4 days, during which the color turns orange and the solution was evaporated under reduced pressure to about 30 mL. The pale-yellow precipitate was isolated and collected by filtration, washed with Et_2O, and dried in air (yield 4.2 g, 60.0%). Anal. Calcd for $C_{39}H_{37}Cl_2N_6O_{2.5}$: C, 66.85; H, 5.32; N, 11.99%. Found: C, 66.99; H, 5.31; N, 11.88%. ESI-MS (MeOH): m/z = 691.2356 (100%) (Fig. S1, ESI†). Calcd for ($H_2L + H^+$) = 691.2355 (100%). ^{1}H NMR (d_6-DMSO): 8.52 (d, 4H), 7.73 (t, 4H), 7.31 (m, 4H), 7.27 (s, 2H) (py protons); 7.07 (s, 2H), 6.98 (s, 2H) (phenyl H); 3.90 (s, 2H) (ph-CH_2-ph); 3.78 (s, 8H) (py-CH_2-N); 3.74 (s, 2H) (ph-CH_2-N). ^{13}C NMR: 157.0, 153.3, 148.1, 136.3, 128.3 (pyridyl C); 128.0, 126.9, 124.1, 122.4, 121.8, 120.7 (phenyl C); 57.5 (N-CH_2-py); 54.6 (N-CH_2-phenyl); 28.5 (phenyl-CH_2-phenyl) (Fig. S2, ESI†). Selected IR (cm^{-1}): 3210 (b, vw) ν_{O-H} (H_2O); 3050 (vw), 3008 (vw), 2914 (vw), 2808 (w) ν_{C-H} (C–H stretching of aliphatic and aromatic groups); 1599 (s), 1569 (m) 1472 (s) 1428 (vs) bis(pyridyl); 1374 (m), 1360 (m), 1292 (m), 1262 (m), 1229 (vs), 1123 (w), 1040 (w), 1002 (m), 970 (m), 886 (m), 766 (vs), 740 (vs), 682 (s) (phenolate and pyridyl groups). UV (MeOH): λ_{max}, nm (ε, M^{-1} cm^{-1}): 213 (2.724×10^4), 262 (1.161×10^4), 294 (5.32×10^3).

$[Mn_2(HL)(\mu_{1,2}\text{-}CH_3COO)_2]PF_6$ (1). A mixture of 6,6′-methylenebis(2-((bis(pyridin-2-ylmethyl)amino)methyl)-4-chlorophenol)hemihydrate (140 mg, 0.2 mmol), Et_3N (40.5 mg, 0.4 mmol) and $Mn(CH_3COO)_2{\cdot}4H_2O$ (69.2 mg, 0.40 mmol) was dissolved in MeOH (20 mL) and heated on a steam-bath for 5 min and this was followed by the addition of NH_4PF_6 (65.2 mg, 0.40 mmol), filtered through Celite, and then allowed to crystallize at room temperature. After 2 hours, the isolated shiny colorless single crystals were collected by filtration, washed with propan-2-ol, Et_2O and air dried (overall yield: 148 mg, 69.5% based on H_2L). Characterization: $C_{43}H_{41}Cl_2F_6Mn_2N_6O_6P$ (MM = 1063.57 g mol^{-1}): calcd: C, 48.56; H, 3.89; N, 7.90%. Found: C, 48.61, H, 3.87; N, 7.91%. ESI-MS (CH_3CN): m/z = 889.0913 (100%). calcd: 889.1277 {$C_{42}H_{41}Cl_2Mn_2N_6O_5$═[$Mn_2$(HL)($CH_3$-COO)($CH_3O$)]$^+$═[$Mn_2$(HL)($\mu_{1,2}$-$CH_3COO)_2$]–CO} (Fig. 1). Selected IR bands (cm^{-1}): 2929 (vw) ν(C–H); 1601 (s), 1572 (m), 1471 (m), 1415 (s) (pyridyl groups: $\nu_{C=C}$, $\nu_{C=N}$); 1293 (w), 1242 (w), 1049 (m), 1013 (m) (phenolate and pyridyl groups); 833 (vs) ν(P–F); 757 (m), 634 (m), 556 (s). UV-Vis: λ_{max}, nm (ε_{max} M^{-1} cm^{-1} per Mn atom) MeOH: 510 (sh, w), 465 (vw), ~650 (11.0); DMSO: 265 (5730), 314 (2635); CH_3CN: 258 (6470), 311 (2850). Molar conductivity: Λ_M (MeOH) = 134.6 Ω^{-1} cm^2 mol^{-1} and Λ_M (CH_3CN) = 139.6 Ω^{-1} cm^2 mol^{-1}.

$[Cu_4(HL)_2(ClO_4)_3(H_2O)_5](ClO_4)_3{\cdot}5H_2O$ (2). A mixture of 6,6′-methylenebis(2-((bis(pyridin-2-ylmethyl)amino)methyl)-4-chlorophenol)hemihydrate (175 mg, 0.25 mmol), Et_3N (50.5 mg, 0.5 mmol) and $Cu(ClO_4)_2{\cdot}6H_2O$ (0.190 g, 0.5 mmol) were dissolved in MeOH (20 mL) and heated on a steam-bath for 5 min. The resulting green solution was filtered through Celite and allowed to crystallize at room temperature. After 3 days, the separated well-shaped green crystals were collected by filtration, washed with propan-2-ol, Et_2O and dried in air (overall yield: 0.325 g, 54.3%). Characterization: $C_{78}H_{90}Cl_{10}Cu_4N_{12}O_{38}$ (MM = 2412.321 g mol^{-1}). calcd: C, 38.84; H, 3.76; N, 6.97%. Found: C, 38.77; H, 3.65; N, 6.94%. ESI-MS (CH_3CN): m/z = 950.9935 (66.91%) (Fig. S3, ESI†). calcd: 951.0358 (100%) for $CuL(ClO_4)_2$ fragment. Selected IR bands (cm^1): 3460 (w, b) (ν_{O-H}, H_2O); 3049 (vw), 3025 (vw), 2919 (vw), 2830 (vw) ν(C–H); 1610 (s), 1562 (w), 1482 (w), 1444 (s) (pyridyl groups: $\nu_{C=C}$, $\nu_{C=N}$); 1073 (vs, b) ν(Cl–O); 1287 (w), 1239 (w), 860 (m), 759 (s). UV-Vis λ_{max}, nm (ε_{max} M^{-1} cm^{-1} per Cu atom) (CH_3CN): 714 (123.3). Λ_M (CH_3CN) = 243.5 Ω^{-1} cm^2 mol^{-1}.

$[Cu_2(H_2L)(NO_3)_2(H_2O)_2](NO_3)_2$ (3). This complex was synthesized essentially as described for **2**, except $Cu(NO_3)_2{\cdot}3H_2O$ was used instead of $Cu(ClO_4)_2{\cdot}6H_2O$. The complex was isolated as light navy-blue crystals, which were not good enough for X-ray structural determination. Characterization: $C_{39}H_{40}Cl_2Cu_2$-$N_{10}O_{16}$ (MM = 1102.790 g mol^{-1}): calcd C, 42.48; H, 3.66; N, 12.70%. Found: C, 42.30; H, 3.33; N, 12.59%. ESI-MS (CH_3CN): m/z = 941.0510 (50.76%) (Fig. S4, ESI†). calcd: 941.0704 (100%) for $HCu_2(H_2L)(NO_3)_2$ fragment. Selected IR bands (cm^1): 3440 (w, b) (ν_{O-H}, H_2O); 3036 (vw), 2923 (vw) ν(C–H); 1608 (m), 1572 (w), 1480 (s), 1438 (s) (pyridyl groups: $\nu_{C=C}$, $\nu_{C=N}$); 1287 (s), 1275 (vs) ν(N–O) (NO_3^-); 1156 (w), 1097 (m), 1009 (s), 857 (m), 770 (vs), 725 (s), 655 (m). UV-Vis λ_{max}, nm (ε_{max} M^{-1}cm^{-1} per Cu atom): CH_3OH: 449 (137.5), 655 (90.3); CH_3CN: 438 (229.9), 562 (148.9); acetone (saturated): 328, 433, 656 (b). Molar conductivity, Λ_M (CH_3OH) = 201.6 Ω^{-1} cm^2 mol^{-1} and Λ_M (CH_3CN) = 199.2 Ω^{-1} cm^2 mol^{-1}.

***Catena*-$[Cu_4(HL)_2(\mu_{1,1}\text{-}N_3)_2(\mu_{1,3}\text{-}N_3)_2](NO_3)_2{\cdot}5H_2O$ (4).** To a mixture containing 6,6′-methylenebis(2-((bis(pyridin-2-ylmethyl)-amino)methyl)-4-chlorophenol)hemihydrate (175 mg, 0.25 mmol), Et_3N (50.5 mg, 0.5 mmol) and $Cu(NO_3)_2{\cdot}3H_2O$ (122 mg, 0.5 mmol) dissolved in MeOH (25 mL), an aqueous solution (5 mL) of NaN_3 (16 mg, 0.25 mmol) was added drop by drop and the resulting green solution was heated on a steam-bath for 5 min, then filtered through Celite and allowed to stand at room temperature. The icy green crystals which separated after 3 days were collected by filtration, washed with propan-2-ol, Et_2O and dried in air (overall yield: 285 mg, 57%). Characterization: $C_{78}H_{80}Cl_4Cu_4N_{26}O_{15}$ (2017.630 g mol^{-1}): calcd: C, 46.43; H, 4.00; N, 18.05%. Found: C, 46.10; H, 3.72; N, 17.69%. ESI-MS (CH_3CN): m/z = 941.0512 (88.32%) (Fig. S5, ESI†). calcd: 941.1067 (100%) for $Cu_2(HL)(N_3)_3$. Selected IR bands (cm^{-1}): 3390 (w, b) ν(O–H); 2042 (vw), 2928 ν(C–H); 2040 (s), 2022 (m) $\nu(N_3)$; 1607 (s), 1572 (m), 1465 (w), 1439 (s) (pyridyl groups: $\nu_{C=C}$, $\nu_{C=N}$); 1322 (s, b) ν(N–O) (NO_3^-); 1237 (m), 1155 (w), 1100 (m), 1051 (m), 1028 (m), 1010 (m), 871 (w), 860 (s), 764 (vs), 725 (vs), 677 (w). UV-Vis: λ_{max}, nm (CH_3CN, saturated): 392, 655; molar conductivity: Λ_M (CH_3OH) = 127.5 Ω^{-1} cm^2 mol^{-1}.

$[Zn_2(HL)(\mu_{1,2}\text{-}OAc)(H_2O)_{0.75}(MeOH)_{0.25}](PF_6)_2{\cdot}0.45(H_2O)$ (5). To a mixture containing 6,6′-methylenebis(2-((bis(pyridin-2-ylmethyl)amino)methyl)-4-chlorophenol)hemihydrate (175 mg, 0.25 mmol), Et_3N (50.5 mg, 0.5 mmol) and $Zn(CH_3COO)_2{\cdot}2H_2O$ (109 mg, 0.50 mmol) dissolved in MeOH (20 mL), NH_4PF_6 (83 mg, 0.50 mmol) was added, and the resulting solution was heated on a steam-bath for 10 min, filtered through Celite and then allowed to crystallize at room temperature. In the following day, the isolated colorless crystals were collected by

filtration, washed with propan-2-ol, Et_2O and air dried (overall yield: 247 mg, 82.3% based on H_2L). Characterization: $C_{41.25}H_{41.40}Cl_2F_{12}N_6O_{5.45}P_2Zn_2$ (MM = 1200.001 g mol^{-1}): calcd: C, 41.29; H, 3.48; N, 7.00%. Found: C, 40.86, H, 3.39; N, 6.98%. ESI-MS (CH_3CN): m/z = 865.0564 (100%) (Fig. S6, ESI†). Calcd = 865.0990 (87.1%) {$C_{40}H_{39}Cl_2N_6O_4Zn_2$═[$Zn_2$(L)($CH_3O$)($H_2O$)]$^+$═[$Zn_2$(HL)($\mu_{1,2}$-$CH_3COO$)($H_2O$)]$^{2+}$–HCO}. Selected IR bands (cm^{-1}): 3582 (w, b) ν(O–H); 2927 (vw) ν(C–H); 1608 (m), 1500 (m), 1444 (m) (pyridyl groups: $\nu_{C=C}$, $\nu_{C=N}$); 1239 (m), 1104 (w), 1022 (m), 757 (m), 732 (m) (phenolate and pyridyl groups); 829 (vs) ν(P–F); UV-Vis: λ_{max}, nm (ε_{max} M^{-1}cm^{-1} per Zn atom) CH_3OH: 211 (16760), 255 (sh), 310 (2390, b). Molar conductivity: Λ_M (CH_3OH) = 271.0 Ω^{-1} cm^2 mol^{-1}.

[Cd_2(HL)($\mu_{1,1,2}$-CH_3COO)(CH_3COO)(H_2O)]PF_6·H_2O (6). A mixture of 6,6′-methylenebis(2-((bis(pyridin-2-ylmethyl)amino)methyl)-4-chlorophenol)hemihydrate (140 mg, 0.2 mmol), Et_3N (40.5 mg, 0.4 mmol), $Cd(NO_3)_2$·$4H_2O$ (123 mg, 0.40 mmol) and sodium acetate, CH_3COONa (54.4 mg, 0.40 mmol) dissolved in MeOH (20 mL) was treated with NH_4PF_6 (130 mg, 0.80 mmol) and the mixture was heated on a steam-bath for 10 min. The resulting solution was then filtered through Celite and allowed to crystallize at room temperature. After 2 days, the white crystals, which separated, were collected by filtration, washed with propan-2-ol, Et_2O and air dried (overall yield: 278 mg, 91.6% based on H_2L). Shiny single crystals suitable for X-ray analysis were obtained upon further recrystallization from MeOH. Characterization: $C_{43}H_{45}Cd_2Cl_2F_6N_6O_8P$ (MM = 1214.55 g mol^{-1}) calcd: C, 42.52; H, 3.73; N, 6.92%. Found: C, 43.01, H, 3.76; N, 6.97%. ESI-MS (CH_3CN): m/z = 1005.0208 (100%) (Fig. S7, ESI†). Calcd = 1005.067 (53%) {$C_{42}H_{42}Cd_2Cl_2N_6O_5$═[$Cd_2$(L)($\mu_{1,1,2}$-$CH_3COO$)-($CH_3$)($H_2O$)]$^+$═[$Cd_2$(HL)($\mu_{1,2}$-$CH_3COO$)($\mu_{1,1,2}$-$CH_3COO$)($H_2O$)]$^+$–$HCO_2$}. Selected IR bands (cm^{-1}): 3612 (w, b) ν(O–H) H_2O); 2929 (vw) ν(C–H); 1603 (m), 1553 (m), 1468 (m), 1421 (m) (pyridyl groups: $\nu_{C=C}$, $\nu_{C=N}$); 1310 (w), 1237 (w), 1049 (m), 1156 (m) (phenolate and pyridyl groups); 836 (vs) ν(P–F); 770 (s), 755 (s), 670 (m). UV-Vis λ_{max}, nm (ε_{max} M^{-1}cm^{-1} per Cd atom) (CH_3OH): 209 (23070), 259 (sh), 312 (2720); DMSO: 263 (7550), 317 (2810); molar conductivity: Λ_M (CH_3OH) = 152.6 Ω^{-1} cm^2 mol^{-1}.

[Cu_2(HL)(CH_3COO)(CH_3OH)][PF_6)$_2$ (7). The complex was isolated as light navy-blue crystals and synthesized using a procedure similar to that described for complex **1** (overall yield: 55.6%). Characterization: $C_{42}H_{42}Cl_2Cu_2F_{12}N_6O_5P_2$ (MM = 1198.746 g mol^{-1}): calcd: C, 42.08; H, 3.53; N, 7.01%. Found: C, 42.24, H, 3.62; N, 6.99%. ESI-MS: m/z = 861.0639 (68.35%) (Fig. S8, ESI†). calcd: m/z = 861.1209 {$C_{41}H_{41}Cl_2Cu_2N_6O_3$═[$Cu_2$(L)($CH_3$)($CH_3OH$)]$^+$═[$Cu_2$(HL)($\mu_{1,2}$-$CH_3COO$)($CH_3OH$)]$^{2+}$–$HCO_2$}. Selected IR bands (cm^{-1}): 3095 (vw), 2931 (vw) ν(C–H); 1600 (m), 1583 (s), 1440 (m), 1446 (m) (pyridyl groups: $\nu_{C=C}$, $\nu_{C=N}$); 1395(s),1 1337 (m), 1302 (w), 1241 (w), 1241 (w), 1162 (w), 1101 (w), 1031 (w), 764 (s); 832 (vs) ν(P–F). UV-Vis λ_{max}, nm (ε_{max} M^{-1}cm^{-1} per Cu atom) (CH_3OH): 431 (213.8), 641 (115.8). Molar conductivity: Λ_M (CH_3OH) = 187.3 Ω^{-1} cm^2 mol^{-1}.

[Cu_2(HL)($NCS)_2$]NO_3·$2H_2O$ (8). Teal colored (overall yield 76.7%). Characterization: $C_{41}H_{39}Cl_2Cu_2N_9O_7S_2$ (MM = 1013.932 g mol^{-1}): calcd: C, 47.72; H, 3.81; N, 12.22%. Found: C, 48.06; H, 3.74; N, 12.19%. ESI-MS: m/z = 874.0438 (66.95%) (Fig. S9, ESI†). calcd: m/z = 874.0620 (100%) for Cu_2(H_2L)(NCS). Selected IR bands (cm^1): 3485 (w, b) (ν_{O-H}, H_2O); 2944 (vw), 2902 (vw) ν(C–H); 2083 (vs) ν(NCS); 1608 (s), 1572 (m), 1450 (m), 1445 (s) (pyridyl groups: $\nu_{C=C}$, $\nu_{C=N}$); 1334 (vs), 1287 (m) ν(N–O) (NO_3^-); 1241 (m), 1100 (m), 1031 (m), 977 (m), 857 (s), 758 (vs), 727 (s), 676 (m). UV-Vis λ_{max}, nm (ε_{max} M^{-1} cm^{-1} per Cu atom) (CH_3OH): 370 (914.8), 641 (160.7); (CH_3CN, saturated) λ_{max}, nm: 215 (s, sh), 374 (m), 483 (sh), 643 (w, b). Molar conductivity, Λ_M (CH_3OH) = 135.4 Ω^{-1} cm^2 mol^{-1}.

Crystallography

The X-ray single-crystal data of title compounds **1**, **4**, **5** and **6** were collected on a Bruker-AXS APEX II CCD diffractometer at 100(2) K. The crystallographic data, conditions retained for the

Table 2 Crystallographic data and processing parameters of **1**, **4**, **5** and **6**

Compound	**1**	**4**	**5**	**6**
Empirical formula	$C_{43}H_{41}Cl_2F_6Mn_2N_6O_6P$	$C_{39}H_{34}Cl_2Cu_2N_{13}O_7$	$C_{41.24}H_{41.39}Cl_2F_6N_6O_{5.45}P_2Zn_2$	$C_{43}H_{45}Cd_2Cl_2F_6N_6O_8P$
Formula mass	1063.57	998.80	1200.00	1214.52
System	Monoclinic	Monoclinic	Triclinic	Monoclinic
Space group	$P2_1/n$	$P2_1/n$	$P\bar{1}$	$P2_1/n$
a (Å)	11.8542(7)	14.4530(8)	13.7082(6)	17.1145(9)
b (Å)	25.7848(14)	23.7277(15)	13.8145(6)	14.5430(7)
c (Å)	16.0771(9)	25.4316(16)	14.4212(6)	20.9676(10)
α (°)	90	90	77.240(2)	90
β (°)	105.415(2)	102.888(3)	69.673(2)	102.122(3)
γ (°)	90	90	72.143(2)	90
V (Å^3)	4737.3(5)	8501.7(9)	2417.44(18)	5102.4(4)
Z	4	8	2	4
T (K)	100(2)	100(2)	100(2)	100(2)
μ (mm^{-1})	0.756	1.397	1.267	1.031
D_{calc} (Mg m^{-3})	1.491	1.561	1.649	1.581
θ max (°)	25.499	26.000	25.499	27.515
Data collected	62 811	141 439	61 834	141 635
Unique refl./R_{int}	8827/0.1089	16 649/0.0946	9010/0.0647	11 704/0.0728
Parameters/restraints	601/0	1147/84	722/104	623/0
Goodness-of-fit on F^2	1.030	1.101	1.065	1.025
$R1$/w$R2$ (all data)	0.0462/0.1372	0.0827/0.1907	0.0641/0.1864	0.0393/0.0749

intensity data collection and some features of the structure refinements are listed in Table 2. Data collections were performed under Mo-Kα radiation (λ = 0.71073 Å); data processing, Lorentz-polarization and absorption corrections were performed using APEX and the SADABS computer programs.[48] The structures were solved using direct methods and refined by full-matrix least-squares methods on F^2, using the SHELX program library.[49] Further programs used: Mercury and PLATON.[50]

Magnetic measurements

The temperature dependent magnetic susceptibilities were measured over the temperature range 2–300 K in a magnetic field of 0.5 T using a Quantum Design MPMS-7 magnetometer at the Institute for Molecular Science (IMS). The measured data were corrected for diamagnetic contributions.[51]

Conclusions

The novel bicompartmental ligand, $H_2L{\cdot}\frac{1}{2}H_2O$ with two phenolate moieties separated by a methylene group, bearing two flexible bis(2-picolyl)amine arms can accommodate two metal(II) ions. This was demonstrated in the isolation of the dinuclear complexes $[Mn_2(HL)(\mu_{1,2}\text{-}OAc)_2]PF_6$ (**1**), $[Cu_2(HL)(ClO_4)_2(H_2O)_2]ClO_4{\cdot}3H_2O$ (**2**), $[Cu_2(H_2L)(NO_3)_2(H_2O)_2](NO_3)_2$ (**3**) $[Zn_2(HL)(\mu_{1,2}\text{-}OAc)(H_2O)_{0.75}(MeOH)_{0.25}](PF_6)_2{\cdot}0.45(H_2O)$ (**5**), $[Cd_2(HL)(\mu_{1,1,2}\text{-}OAc)(OAc)(H_2O)]PF_6{\cdot}H_2O$ (**6**), $[Cu_2(HL)(OAc)(CH_3OH)](PF_6)_2$ (**7**) and $[Cu_2(HL)(NCS)_2]NO_3{\cdot}2H_2O$ (**8**). The metal centers act magnetically independent of each other as in complex **2** and probably **3**. However, in the presence of small bridging ligands such as acetate anions, complexes **1**, **5** and **6** were isolated and structurally characterized, in which the OAc^- ligands link the two metal ions in the $\mu_{1,2}$- or $\mu_{1,1,2}$-OAc bonding modes. In addition, using the versatile bonding azide ligand, polymeric bridged-azido tetranuclear *catena*-$[Cu_4(HL)_2(\mu_{1,1}\text{-}N_3)_2(\mu_{1,3}\text{-}N_3)_2](NO_3)_2{\cdot}5H_2O$ (**4**) was obtained. In these complexes and with the exception of **3**, only monoprotonated HL^- ligand was coordinated to metal ions, whereas fully protonated H_2L was found in **3**. This was attributed to the strong hydrogen bonds generated from the deprotonated and protonated phenolates, phO···H···Oph. The magnetic susceptibility measurements in the latter complex revealed very weak antiferromagnetic (AF) coupling through the di-$\mu_{1,1}$-N_3-bridged and moderate-to-strong AF coupling through the di-$\mu_{1,3}$-N_3-bridged dicopper(II) units. On the other hand, weak AF and negligible ferromagnetic interactions were determined in dimanganese(II) **1** and dicopper(II) **2**, respectively.

Conflicts of interest

The authors declare no conflicts of interest.

Acknowledgements

This research was financially supported by the Department of Chemistry – University of Louisiana at Lafayette, and S. S. M. and F. R. L. are very grateful for this support.

References

1 (*a*) A. Terán, A. Jaafar, A. E. Sánchez-Peláez, M. C. Torralba and Á. Gutiérrez, *J. Biol. Inorg. Chem.*, 2020, **25**, 671–683; (*b*) A. M. Magherusan, D. N. Nelis, B. Twamley and A. R. McDonald, *Dalton Trans.*, 2018, **21**, 15555–15564.

2 (*a*) D. Mukherjee, P. Nag, A. A. Shteinman, S. R. Vennapusa, U. Mandal and M. Mitra, *RSC Adv.*, 2021, **11**, 22951–22959; (*b*) R. R. Tripathy, S. Singha and S. Sarkar, *J. Coord. Chem.*, 2022, **75**, 1967–2017.

3 L. J. Daumann, J. A. Larrabee, P. Comba, G. Schenk and L. R. Gahan, *Eur. J. Inorg. Chem.*, 2013, 3082–3089.

4 K. D. Karlin, Z. Tyeklár, A. Farooq, M. S. Haka, P. Ghosh, R. W. Cruse, Y. Gultneth, J. C. Hayes, P. J. Toscano and J. Zubieta, *Inorg. Chem.*, 1992, **31**, 1436–1451.

5 (*a*) S. Cao, R. Cheng, D. Wang, Y. Zhao, R. Tang, X. Yang and J. Chen, *J. Inorg. Biochem.*, 2019, **192**, 126–139; (*b*) G. A. dos Santos Silva, A. L. Amorim, B. de Souza, P. Gabriel, H. Terenzi, E. Nordlander, A. Neves and R. A. Peralta, *Dalton Trans.*, 2017, **46**, 11380–11394.

6 S. S. Massoud, F. R. Louka, W. Xu, R. S. Perkins, R. Vicente, J. H. Albering and F. A. Mautner, *Eur. J. Inorg. Chem.*, 2011, 3469–3479.

7 S. S. Massoud, C. C. Ledet, T. Junk, S. Bosch, P. Comba, R. Herchel, J. Hošek, Z. Trávníček, R. C. Fischer and F. A. Mautner, *Dalton Trans.*, 2016, **45**, 12933–12950.

8 (*a*) C. Pathak, D. Kumar, M. K. Gangwar, D. Mhatre, T. Roisnel and P. Ghosh, *J. Inorg. Biochem.*, 2018, **185**, 30–42; (*b*) S. K. Barman, T. Mondal, K. Debasis, F. Lloret and R. Mukherjee, *Dalton Trans.*, 2017, **46**, 4038–4054; (*c*) L. Tjioe, T. Joshi, C. M. Forsyth, B. Moubaraki, K. S. Murray, J. Brugger, B. Graham and L. Spiccia, *Inorg. Chem.*, 2012, **51**, 939–953.

9 (*a*) C. Pathak, S. K. Gupta, M. K. Gangwar, A. P. Prakasham and P. Ghosh, *ACS Omega*, 2017, **2**, 4737–4750; (*b*) A. Neves, M. Lanzanaster, A. J. Bortoluzzi, R. A. Peralla, A. Cassellato, E. E. Castellano, P. Herrald, M. J. Riley and G. Schenk, *J. Chem. Soc.*, 2007, **129**, 7486–7487.

10 S. S. Massoud, F. R. Louka, N. M. H. Salem, R. C. Fischer, A. Torvisco, F. A. Mautner, J. Vančo, J. Belza, Z. Dvořák and Z. Trávníček, *Eur. J. Med. Chem.*, 2023, **246**, 114992, DOI: 10.1016/j.ejmech.2022.114992.

11 (*a*) D. Maiti, D. H. Lee, K. Gaoutchenova, C. Wurtele, M. C. Holthausen, A. A. N. Sarjeant, J. Sundermeyer, S. Schindler and K. D. Karlin, *Angew. Chem., Int. Ed.*, 2008, **47**, 82–85; (*b*) L. Li, N. N. Murthy, J. Tesler, L. N. Zakharov, G. P. A. Yap, A. L. Rheingold, K. D. Karlin and S. E. Rokita, *Inorg. Chem.*, 2006, **45**, 7144–7159; (*c*) C. Kim, Y. Dong and L. Que Jr., *J. Am. Chem. Soc.*, 1997, **119**, 3635–3636; (*d*) J. A. Halfen, J. S. Mahapatra, E. C. Wilkinson, S. Kaderli, V. C. Yong, Jr., L. Que, A. D. Zuberbuhler and W. B. Tolman, *Science*, 1996, **271**, 1397–1400.

12 (*a*) A. Gutierrez, M. F. Perpiñán, A. E. Sanchez, A. C. Torralba and V. González, *Inorg. Chim. Acta*, 2016, **453**, 169–178; (*b*) Y. Gultneh, T. B. Yisgedu, Y. T. Tesema and R. J. Butcher, *Inorg. Chem.*, 2003, **42**, 1857–1867; (*c*) S. Itoh,

H. Bandoh, S. Nagatomo, T. Kitagawa and S. Fukuzumi, *J. Am. Chem. Soc.*, 1999, **121**, 8945–8946; (*d*) S. V. Kryalov and E. V. Rybak-Akimova, *Dalton Trans.*, 1999, 3335–3336.

13 (*a*) Y. Zhang, D. Yang, Y. Li, X. Zhao, B. Wang and J. Qu, *Catal. Sci. Technol.*, 2019, **9**, 6492–6502; (*b*) R. Bikas, F. Shahmoradi, N. Noshiranzadeh, M. Emami and S. Reinoso, *Inorg. Chim. Acta*, 2017, **466**, 100–109; (*c*) P. Gamez, P. de Hoog, M. Lutz, A. L. Spek and J. Reedijk, *Inorg. Chim. Acta*, 2003, **351**, 319–325.

14 (*a*) G. Li, D. Zhu, X. Wang, Z. Su and M. R. Bryce, *Chem. Soc. Rev.*, 2020, **49**, 765–838; (*b*) J.-W. Wang, D.-C. Zhong and T. B. Lu, *Coord. Chem. Rev.*, 2018, **377**, 225–236.

15 (*a*) A. Valizadel, R. Bikas, P. Aleshkevych, A. Kozakiecwicz, S. I. Allakhverdiev and M. M. Najafpour, *Int. J. Hydrogen Energy*, 2021, **46**, 29896–29904; (*b*) Y. Xu, A. Fischer, L. Duan, L. Tong, E. Gabrielsson, B. Åkermark and L. Sun, *Angew. Chem., Int. Ed.*, 2010, **122**, 9118–9121; (*c*) P. A. Goodson, A. R. Oki, J. Glerup and D. J. Hodgson, *J. Am. Chem. Soc.*, 1990, **112**, 6248.

16 R. Modak, B. Mondal, Y. Sikdar, J. Banerjee, E. Colacio, I. Oyarzabal, J. Cano and S. Goswami, *Dalton Trans.*, 2020, **49**, 6328–6340.

17 (*a*) S. S. Tandon, S. D. Bunge, N. Patel, E. C. Wang and L. K. Thompson, *Molecules*, 2020, **25**, 5549, DOI: **10.3390/molecules25235549**; (*b*) D. Venegas-Yazigi, D. Aravena, E. Spodine, E. Ruiz and S. Alvarez, *Coord. Chem. Rev.*, 2010, **254**, 2086–2095.

18 (*a*) S. S. Massoud, F. R. Louka, M. T. Dial, N. M. H. Salem, R. C. Fischer, A. Torvisco, F. A. Mautner, K. Nakashima, M. Handa and M. Mikuriya, *Molecules*, 2023, **28**, 2648, DOI: **10.3390/molecules28062648**; (*b*) Y. Kakuta, N. Masuda, M. Kurushima, T. Hashimoto, D. Yoshioka, H. Sakiyama, Y. Hiraoka, M. Handa and M. Mikuriya, *Chem. Papers*, 2014, **68**, 923–931.

19 S. S. Massoud, T. Junk, F. R. Louka, R. Herchel, Z. Travnicek, R. C. Fischer and F. A. Mautner, *RSC Adv.*, 2015, **5**, 87139–87150.

20 S. S. Massoud, T. Junk, M. Mikuriya, Y. Naka and F. A. Mautner, *Inorg. Chem. Commun.*, 2014, **50**, 48–50.

21 (*a*) S. Sakamoto, T. Fujinami, K. Nishi, N. Matsumoto, N. Mochida, T. Ishida, Y. Sunatsuki and N. Re, *Inorg. Chem.*, 2013, **52**, 7218–7229; (*b*) K. Ehama, Y. Omichi, S. Sakamoto, T. Fujinami, N. Matsumoto, N. Mochida, T. Ishida, Y. Sunatsuki and M. Tsuchimoto, *Inorg. Chem.*, 2013, **52**, 12828–12841; (*c*) S. Sakamoto, S. Yamauchi, H. Hagiwara, N. Matsumoto, Y. Sunatsuki and N. Re, *Inorg. Chem. Commun.*, 2012, **26**, 20–23.

22 (*a*) S. Titos-Padilla, J. Ruiz, J. M. Herrera, K. Euan, E. K. Brechin, W. Wersndorfer, F. Lloret and E. Colacio, *Inorg. Chem.*, 2013, **52**, 9620–9626; (*b*) E. Colacio, J. Ruiz, A. J. Mota, M. A. Palacios, E. Cremades, E. Ruiz, F. J. White and E. K. Brechin, *Inorg. Chem.*, 2012, **51**, 5857–5868.

23 (*a*) F. A. Mautner., F. R. Louka, T. Le Guet and S. S. Massoud, *J. Mol. Struct.*, 2009, **919**, 196–203; (*b*) T. LeGuet, F. A. Mautner, S. Demeshko, F. Meyer, R. S. Perkins and S. S. Massoud, *Inorg. Chem. Commun.*, 2009, **12**, 321–324.

24 (*a*) F. R. Louka, M. L. Spell, J. Grebowicz, J. H. Albering, F. A. Mautner and S. S. Massoud, *J. Mol. Struct.*, 2011, **995**, 103–108; (*b*) F. A. Mautner, J. H. Albering, R. Vicente, F. R. Louka, A. A. Gallo and S. S. Massoud, *Inorg. Chim. Acta*, 2011, **365**, 290–296.

25 S. S. Massoud, M. Spell, C. Ledet, T. Junk, R. Herchel, R. C. Fischer, Z. Travnicek and F. A. Mautner, *Dalton Trans.*, 2015, **44**, 2110–2121.

26 (*a*) *In Bioinorganic Chemistry of Copper Chapman and Hall* ed. K. D. Karlin and Z. Tyeklár, New York, 1993; (*b*) K. D. Karlin, A. Farooq, J. C. Hayes, B. I. Cohen, T. M. Rowe, E. Sinn and J. Zubieta, *Inorg. Chem.*, 1987, **26**, 1271–1280.

27 S. S. Massoud, J. Junk, R. Herchel, Z. Travnicek, M. Mikuriya, R. C. Fischer and F. A. Mautner, *Inorg. Chem. Commun.*, 2015, **60**, 1–3.

28 F. A. Mautner, F. R. Louka, J. Hofer, M. Spell, A. Lefèvre, A. E. Guilbeau and S. S. Massoud, *Cryst. Growth Des.*, 2013, **13**, 4518–4525.

29 F. A. Mautner, J. B. Soileau, P. K. Bankole, A. Gallo and S. S. Massoud, *J. Mol. Struct.*, 2008, **889**, 271–278.

30 F. A. Mautner., F. R. Louka, T. Le Guet and S. S. Massoud, *J. Mol. Struct.*, 2009, **919**, 196–203.

31 (*a*) S. S. Massoud and F. A. Mautner, *Inorg. Chim. Acta*, 2005, **358**, 3334–3340; (*b*) S. S. Massoud, F. R. Louka, R. N. David, M. J. Dartez, Q. L. Nguyn, N. J. Labry, R. C. Fischer and F. A. Mautner, *Polyhedron*, 2015, **90**, 258–265.

32 F. A. Mautner, R. C. Fischer, A. Torvisco, M. M. Henary, A. Milner, H. De Villier, T. N. V. Karsili, F. R. Louka and S. S. Massoud, *Crystals*, 2019, **9**, 38, DOI: **10.3390/cryst9010038**.

33 B. G. Deacon and R. J. Philips, *Coord. Chem. Rev.*, 1980, **33**, 227–250.

34 (*a*) B. J. Hathaway, in *Comprehensive Coordination Chemistry*, ed. G. Wilkinson, R. D. Gillard, J. A. McCleverty, vol. 5, Pergamon Press, Oxford, England, 1987, p. 533; (*b*) K. Matelková, L. Kucková, A. Mašlejová, J. Moncoľ, V. Jorík and J. Kožíšek, *Chem. Papers*, 2016, **70**, 82–92.

35 (*a*) F. A. Mautner, R. C. Fischer, L. G. Rashmawi, F. R. Louka and S. S. Massoud, *Polyhedron*, 2017, **124**, 237–242; (*b*) S. S. Massoud, R. F. Louka, R. N. David, M. J. Dartez, Q. L. Nguyn, N. J. Labry, R. C. Fischer and F. A. Mautner, *Polyhedron*, 2015, **90**, 258–265; (*c*) F. A. Mautner, R. Vicente, F. R. Louka and S. S. Massoud, *Inorg. Chim. Acta*, 2008, **361**, 1339–1348.

36 B. N. Figgis, Introduction to Ligand Fields, *Intercedence*, Wiley, New York, 1966.

37 (*a*) E. Colacio, J. P. Costes, R. Kivekas, J. P. Laurent, J. Ruiz and M. Sundberg, *Inorg. Chem.*, 1991, **30**, 1475–1479; (*b*) K. J. Oberhausen, J. F. Richardson, R. M. Buchanan, J. K. McCusker, D. N. Hendrickson and J. M. Latour, *Inorg. Chem.*, 1991, **30**, 1357–1365.

38 F. Thomas, G. Gellon, I. Gautier-Luneau, E. Saint-Aman and J.-L. Pierre, *Angew. Chem., Int. Ed.*, 2002, **41**, 3047–3050.

39 A. W. Addison, T. N. Rao, J. Reedijk, J. V. Rijin and G. C. Verschoor, *J. Chem. Soc., Dalton Trans.*, 1984, 1349–1356.

40 M. Mikuriya, T. Fujii, T. Tokii and A. Kawamori, *Bull. Chem. Soc. Jpn.*, 1993, **66**, 1675–1686.
41 H. Sakiyama, A. Suenaga, M. Sakamoto, K. Unoura, K. Inoue and M. Yamasaki, *Inorg. Chim. Acta*, 2000, **310**, 163–168.
42 S. Blanchard, G. Blondin, E. Rivière, M. Nierlich and J.-J. Girerd, *Inorg. Chem.*, 2003, **42**, 4568–4578.
43 S.-B. Yu, S. J. Lippard, H. Shweky and A. Bino, *Inorg. Chem.*, 1992, **31**, 3502–3504.
44 B.-H. Ye, T. Mak, I. D. Williams and X.-Y. Li, *Chem. Commun.*, 1997, 1813–1814.
45 B. E. Schultz, B.-H. Ye, X.-Y. Li and S. L. Chan, *Inorg. Chem.*, 1997, **36**, 2617–2622.
46 I. Romero, L. Debois, M.-N. Collomb, A. Deronzier, J.-M. Latour and J. Pécaut, *Inorg. Chem.*, 2002, **41**, 1795–1806.
47 (*a*) M. Mikuriya, C. Yamakawa, K. Tanabe, R. Nukita, Y. Amabe, D. Yoshioka, R. Mitsuhashi, R. Tatehata, H. Tanaka, M. Handa and M. Tsuboi, *Magnetochemistry*, 2021, **7**, 35, DOI: **10.3390/magnetochemistry7030035**; (*b*) S. Wada, K. Saka, D. Yoshioka and M. Mikuriya, *Bull. Chem. Soc. Jpn.*, 2010, **83**, 364–374, DOI: **10.1246/bcsj.20090284**.
48 (*a*) Bruker SAINT v. 7.23, 2005; Bruker APEX 2, v. 2.0-2, Bruker AXS Inc. Madison, Wisconsin, USA, 2006; (*b*) G. M. Sheldrick, *SADABS v. 2.*, University of Goettingen, Germany, 2001.
49 G. M. Sheldrick, *Acta Crystallogr.*, 2008, **A64**, 112–122.
50 C. F. Macrae, P. R. Edington, P. McCabe, E. Pidcock, G. P. Shields, R. Taylor, T. Towler and J. van de Streek, *J. Appl. Crystallogr.*, 2006, **39**, 453–457.
51 O. Kahn, *Molecular Magnetism*, VCH publishers, New York, 1993.